

# Bifurcation and stability analysis of rotating chemical spirals in circular domains: Boundary-induced meandering and stabilization

Markus Bär,<sup>1</sup> Anil K. Bangia,<sup>2</sup> and Ioannis G. Kevrekidis<sup>2</sup>

<sup>1</sup>Max-Planck-Institut für Physik komplexer Systeme, Nöthnitzer Straße 38, D-01187 Dresden, Germany

<sup>2</sup>Department of Chemical Engineering, Princeton University, Princeton, New Jersey 08544

(Received 18 June 2002; published 27 May 2003)

Recent experimental and model studies have revealed that the domain size may strongly influence the dynamics of rotating spirals in two-dimensional pattern forming chemical reactions. Hartmann *et al.* [Phys. Rev. Lett. **76**, 1384 (1996)], report a frequency increase of spirals in circular domains with diameters substantially smaller than the spiral wavelength in a large domain for the catalytic NO+CO reaction on a microstructured platinum surface. Accompanying simulations with a simple reaction-diffusion system reproduced the behavior. Here, we supplement these studies by a numerical bifurcation and stability analysis of rotating spirals in a simple activator-inhibitor model. The problem is solved in a corotating frame of reference. No-flux conditions are imposed at the boundary of the circular domain. At large domain sizes, eigenvalues and eigenvectors very close to those corresponding to infinite medium translational invariance are observed. Upon decrease of domain size, we observe a simultaneous change in the rotation frequency and a deviation of these eigenvalues from being neutrally stable (zero real part). The latter phenomenon indicates that the translation symmetry of the spiral solution is appreciably broken due to the interaction with the (now nearby) wall. Various dynamical regimes are found: first, the spiral simply tries to avoid the boundary and its tip moves towards the center of the circular domain corresponding to a negative real part of the “translational” eigenvalues. This effect is noticeable at a domain radius of  $R < R_{cr,1}$ . The spiral subsequently exhibits an oscillatory instability: the tip trajectory displays a meandering motion, which may be characterized as *boundary-induced spiral meandering*. A systematic study of the spiral rotation as a function of a control parameter and the domain size reveals that the meandering instability in large domains becomes suppressed, and the spiral rotation becomes rigid, at a critical radius  $R_{cr,0}$ . Boundary-induced meandering arises below a second critical radius  $R_{cr,2} < R_{cr,0}$ .

DOI: 10.1103/PhysRevE.67.056126

PACS number(s): 05.65.+b

## I. INTRODUCTION

Rotating spiral waves constitute one of the most common spatiotemporal patterns observed in two-dimensional non-equilibrium systems. They have been observed experimentally in a wide variety of systems including heterogeneous catalytic reactions (CO+O<sub>2</sub>/Pt, NO+CO/Pt, etc.), liquid phase reactions [such as the famous Belousov-Zhabotinskii (BZ) reaction], slime mold aggregation, and electrical activity on cardiac tissue. Their ubiquitous presence has generated a widespread interest in the study of their dynamical behavior among physicists, biologists, and applied mathematicians [1–7].

The experimental investigations of spiral waves in earlier years almost exclusively concentrated on the BZ system [8,9]. The reaction can be carried out easily in a petri dish (batch) or using a continuous setup. More recently, extensive interesting observations have been made on the CO oxidation system [10]. One motivation for the study of spirals comes from cardiology; the breakup of isolated spiral waves of electrical activity in cardiac tissue into disorganized excitations is deemed to play an important role in fibrillation [4].

Particlelike spiral interaction has been studied in the complex Ginzburg-Landau equation by various authors. Controversial ideas about the range of the interaction force have been published. While early work favored a  $1/r$  decay [11,12], more extensive recent analysis and simulations point

towards an exponential decay [13]. Another important issue deals with formation of symmetric spiral pairs or spontaneous symmetry breaking and decay of one of two spirals in an interaction event. A related problem (the interaction of spirals with a reflecting mirror wall in a circular geometry) has been studied in reaction-diffusion models for excitable media, as we will discuss below. Kinematical theory predicts a  $1/r$  correction to the rotation frequency [14], while a different approach yields a superexponential correction [15].

Experiments on a catalytic surface in small circular domains and corresponding simulations are documented in Ref. [17]. Additional information is provided by a recent experimental report [18]. These studies show a particular strong effect of the domain size on the spiral’s rotation frequency for weak excitability where the kinematic theory is valid. Simulations in this regime show a  $1/r$  correction, see Ref. [17], as predicted by kinematical arguments [14]. The superexponential effects in the limit of high excitability [15] predict only weak changes in the rotation frequency. All theoretical results are based on some oversimplification of realistic models. Numerical simulation can give an approximate picture, but more accurate results can be obtained by means of numerical stability analysis of spirals as shown below. In this paper, we focus on qualitative changes of spiral wave behavior rather than on quantitative predictions in the cited articles. This is achieved by employing numerical bifurcation and stability analysis rather than with direct simulations (see the Ref. [16] for a more detailed presentation). In particular, we find that simple rotating spirals are

destabilized due to boundary effects for small domains (*boundary-induced meandering*), while spiral meandering is suppressed at intermediate domain sizes. Before we enter into the topic of numerical stability analysis of spirals in small domains, we review briefly the general properties of rotating spirals in Sec. II and provide a description of the methodology in Sec. III. In Sec. IV, results on the boundary-induced meandering at small domain sizes are presented, while Sec. V deals with the restabilization of large domain meandering spirals at intermediate domain sizes. A brief discussion in the last section concludes the paper.

## II. DYNAMICS OF ROTATING SPIRALS

Most theoretical studies of spiral waves have centered around two limiting cases. The free boundary approach was first introduced by Fife [5,19] and later extensively investigated by others, see Refs. [6,20–25]. A simple kinematic theory in terms of motion of curves was first sketched in 1946 by Wiener and Rosenblueth [26] and later carried out by Zykov and Mikhailov [3,27]. Although the analytical work has contributed to a significant advancement in the understanding of spiral wave behavior, certain aspects of the behavior are better understood through computer-assisted analysis. Numerical investigations of the dynamics of spiral waves have been carried out for a variety of reaction-diffusion systems [28–32].

It is worthwhile to summarize the essential features of the two-parameter bifurcation diagram of spiral wave dynamics in a generic model of excitable media first described by Zykov [1]. The diagram is “generic” in the sense that most two-parameter investigations of spiral dynamics in other excitable systems have shown similar states and transitions. This diagram was obtained by Winfree [2] in a detailed numerical study of the FitzHugh-Nagumo (FHN) equations, which read

$$\partial_t u = \nabla^2 u + u - \frac{u^3}{3} - v, \quad (1)$$

$$\partial_t v = \epsilon(u + \beta - \gamma v). \quad (2)$$

The parameter  $\gamma$  was fixed at 0.5 and numerical simulations were conducted to observe types of spiral wave behavior in the FHN model. The bifurcation or “phase” diagram in the two control parameters  $(\epsilon, \beta)$  is divided into five distinct regions representing different dynamical states, separated by curves of bifurcation loci. When  $\beta$  and  $\epsilon$  are large, no wave propagation is possible in the FHN system. Here the medium is not sufficiently excitable to support waves and all initial conditions evolve to a spatially uniform state. The curve  $\partial P$  denotes the “boundary of propagation”; planar waves exist in the system above this curve. The curve  $\partial R$  denotes the “rotor boundary”; the system supports rotating wave solutions above this curve. A good representation of the dynamics near the  $\partial R$  boundary is the evolution of a broken wave segment of a planar wave [3]. In the region between  $\partial P$  and  $\partial R$ , broken wave tips retract as they propagate along straight lines. Above the  $\partial R$  curve, an initial broken segment curls up

and evolves into a rotating spiral wave. Spirals exist in the region bounded by  $\partial R$  and  $\partial M$  curves, and are characterized by rigid rotation around a fixed point. Tip motions of rigidly rotating spirals form circles. The radius of the tip path, spiral period, and spiral wavelength all diverge as the boundary  $\partial R$  is approached in the parameter space. The curve  $\partial M$  denotes the “meandering boundary” and is associated with the transition from rigidly rotating spirals to meandering motion of the spiral core. Using a similar model of excitable media, Barkley [7] showed that  $\partial M$  is a single smooth locus of Hopf bifurcations of rotating spirals. The tip paths of the meandering spirals (more specifically *modulated rotating waves*) form flowerlike patterns characterized by two temporal frequencies. Finally, the region to the right of the  $\partial C$  curve is characterized by dynamics that are more complicated than two-frequency quasiperiodic, and possibly even chaotic. These states are termed by Winfree as “hypermeandering.”

Although accurate time-dependent numerical simulations constitute a useful tool for analysis, many problems can be tackled more efficiently through detailed linear stability and bifurcation analysis.

## III. COMPUTATIONAL LINEAR STABILITY ANALYSIS OF SPIRALS

Spiral waves are solutions to the governing reaction-diffusion equations with a rotational symmetry; they appear stationary in a frame rotating with the frequency of the wave (for a description of the method used here, see also Ref. [33]). Consequently, they can be computed as steady states of the following reaction-diffusion equations in polar coordinates:

$$\mathbf{0} = \partial_t \mathbf{u} = \mathbf{F}(\mathbf{u}) \equiv \mathbf{f}(\mathbf{u}) + \mathcal{D} \nabla^2 \mathbf{u} + \omega \partial_\theta \mathbf{u}, \quad (3)$$

where  $\mathbf{u} = (u, v)^T$ ,  $\mathcal{D} = \text{diag}(1, 0)$ , and  $\mathbf{f}(\mathbf{u})$  represents the kinetic terms of a modified Barkley model with delayed inhibitory production [28,31],

$$\mathbf{f}(\mathbf{u}) = (-\epsilon^{-1} u(u-1)[u - (v+b)/a], u^3 - v)^T.$$

The last term on the right-hand side of Eq. (3) comes from the rotating frame of reference ( $\omega$  is the appropriate angular velocity). This model is qualitatively similar to the FitzHugh-Nagumo model [Eqs. (1) and (2)], but possesses three fixed points  $\mathbf{u}_0 = (u_0, v_0)^T$  with  $\mathbf{f}(\mathbf{u}) = \mathbf{0}$ . One is the stable rest state  $(u_0, v_0) = (0, 0)$  of the excitable medium, while the two other fixed points (a saddle and a focus) are unstable and result from the repeated intersection of the nullcline curves  $u = (v+b)/a$  and  $u^3 = v$  in the  $u-v$  plane.

The boundary conditions on a circular domain of radius  $R$  are taken to be no flux in the radial direction ( $\partial_r \mathbf{u}|_R = 0$ ). The system defined by Eq. (3) has a continuum of solutions (given by all arbitrary rotations of the spiral) and the additional unknown  $\omega$ . This indeterminacy is removed and a unique steady solution is picked out by fixing the rotational phase of the spiral (here at  $r = R/2, \theta = \pi$ ). This is done by appending an additional pinning condition given by

$$\partial_\theta v|_{r=R/2, \theta=\pi} = 0, \quad (4)$$

which allows for determining the unique value of  $\omega$  along with a *particular* rotation of the spiral shape.

The stability of the steady state  $\bar{\mathbf{u}}$  of Eqs. (3) and (4) with respect to small perturbations is determined by the following linearized eigenvalue problem:

$$DF(\bar{\mathbf{u}})\mathcal{U} = \lambda\mathcal{U}, \quad (5)$$

where

$$DF(\bar{\mathbf{u}}) = D\mathbf{f}(\bar{\mathbf{u}}) + \mathcal{D}\nabla^2 + \omega\partial_\theta, \quad (6)$$

while  $\lambda$  and  $\mathcal{U}$  are the eigenvalues and the eigenmodes of the linearized operator  $DF(\bar{\mathbf{u}})$ . The eigenvalues  $\lambda$  determine the linear stability of the spiral solution; a bifurcation is indicated when a real eigenvalue or a complex conjugate pair of imaginary eigenvalues cross into the right half of the complex plane.

Equations (3) are now discretized on a polar grid, where we can split the Laplace operator in an azimuthal and a radial part  $\nabla^2 u(r, \theta) = \nabla_r^2 u(r, \theta) + \nabla_\theta^2 u(r, \theta)$ . The radial and azimuthal contributions are then given by

$$\nabla_\theta^2 u(r, \theta) = \frac{1}{r^2} \frac{\partial^2}{\partial \theta^2} u(r, \theta), \quad (7)$$

$$\nabla_r^2 u(r, \theta) = \frac{1}{r} \frac{\partial}{\partial r} u(r, \theta) + \frac{\partial^2}{\partial r^2} u(r, \theta). \quad (8)$$

The concentration fields  $u$  and  $v$  are then expanded in Fourier modes in the azimuthal direction and discretized with second-order finite differences to evaluate the operators in the radial direction. The boundary conditions at  $r=R$  are taken to be no-flux in the radial direction  $\partial u((r, \theta)/\partial r)|_{r=R} = 0$ . The boundary condition at  $r=0$  is taken to be zero-flux as well, while the singularity in the first term in Eq. (8) has been treated using l'Hôpital's rule. Spatial discretization yields a set of ordinary differential equations (ODEs) describing the time evolution of coefficients of the discretization of the concentration variables. Most results reported here were obtained by taking  $N_r = 51$  radial grid points and 30 Fourier modes in the azimuthal direction with  $N_\theta = 128$  collocation points. Such a discretization results in a dynamical system of  $\sim 6000$  ODEs.

This system of ODEs is stiff and explicit time integration methods are plagued by stability constraints. We perform transient simulations of the discretized system with the help of the stiff ODE solver ODESSA [35], which employs variable (adaptive) step size with up to fifth-order backward difference formulas.

Dynamical systems of this size are prohibitive for the routine stability and bifurcation algorithms based on direct solvers. We employ large scale, iterative methods that have recently been developed and applied to matrix eigenproblems [36–38]. The steady state problem is solved using Newton's method which can be accelerated by the use of Krylov-based iterative solution methods for linear systems [39]. Pseudo-arclength continuation techniques are then utilized to follow

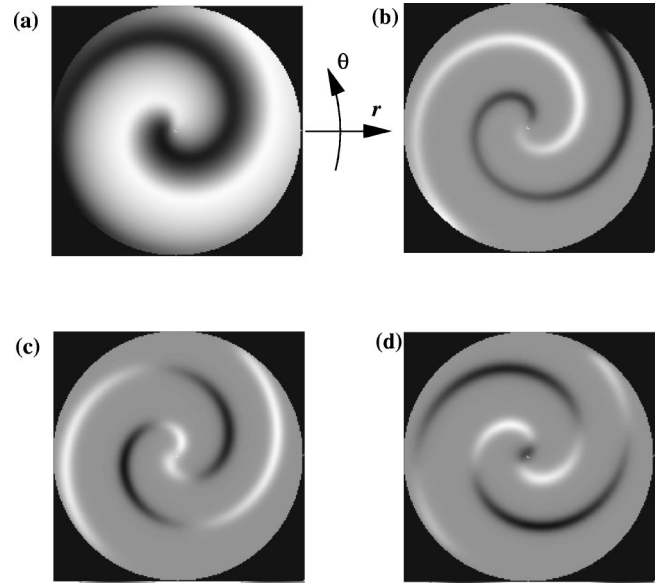


FIG. 1. Eigenmodes due to symmetry [34]: (a)  $v$  concentration field of a rotating spiral wave; the parameters are  $\epsilon = 0.025$ ,  $a = 0.8$ ,  $b = 0.02$ ,  $R = 10$ , (b) eigenmode resulting from rotational symmetry, (c) and (d) real and imaginary parts of the eigenmodes associated with the translational symmetry. The gray scale value represents the variable  $u$ ; darker regions correspond to higher values of  $u$  and vice versa.

the branch of spiral wave solution as the parameter values are varied. This continuation scheme is robust to the presence of folds in the spiral branch and traces the solution branch into parameter regions where the solution is unstable. The stability of the spiral solution is monitored by finding the leading eigenvalue (those with the largest real part, close to the imaginary axis) and corresponding eigenvectors at each continuation step. The leading eigenpairs are computed using an iterative Arnoldi method with implicit deflation [36–38].

At first glance it appears that three of the eigenvalues of the linearized eigenproblem (5) lie on the imaginary axis; they are associated with the symmetries in the infinite, unbounded system. Figure 1 shows the spatial plots of the corresponding eigenmodes. The gray scale value in these plots represents the variable  $u$ . The eigenvalue at zero  $\lambda_R$  arises from the rotational symmetry of the spiral wave. The rotationally symmetric eigenmode can be shown to be simply the azimuthal derivative of the concentration field,  $\mathcal{U}_R = \partial_\theta \bar{\mathbf{u}}$ . Furthermore, a spiral wave in an infinite medium can be arbitrarily translated on the plane. In a frame rotating with the frequency  $\omega$ , this results in a complex eigenpair at  $\lambda_T = \pm i\omega$  [7,34]. The real and complex parts of the corresponding eigenmodes can be shown to be the  $x$  and  $y$  derivatives of the concentration field  $\mathcal{U}_T = \partial_x \bar{\mathbf{u}} \pm i \partial_y \bar{\mathbf{u}}$ . This eigenpair is “descended from” the infinite medium problem, and if the distance between spiral core and boundary is large, the “finite box” eigenvalues have real part very close to zero.

Indeed, the presence of no-flux boundaries in a finite domain at  $r=R$  breaks the translational symmetry of the spiral on the plane. However, for a sufficiently large domain size,

the eigenvalues associated with the translational symmetry are numerically very close to their values for an infinitely extended domain  $\lambda_T = 0 \pm i\omega$  [7]. The deviation of  $\text{Re}(\lambda_T)$  from zero is a measure of how much the boundaries “influence” the spiral core. Thus, the eigenvalues  $\lambda_T$  quantify, in a sense, the interaction of the rotating spiral with the boundary. Since the spiral is centered in the circular domain, any translation will move it towards the boundary and should probe the force between the spiral and the zero-flux boundary, which can be considered a (curved) mirror wall. All other eigenvalues have negative real parts in our study; instability here arises only from the interaction with the boundary expressed in  $\lambda_T$ .

#### IV. SPIRAL INSTABILITY IN SMALL CIRCULAR DOMAINS

Spirals in spatially extended domains select a unique set of values for their frequency  $\omega$  and spatial wavelength  $\lambda$  depending on the control parameters  $\epsilon$ ,  $a$ , and  $b$  in our model, respectively,  $\epsilon$ ,  $\gamma$ , and  $\beta$  in the FHN system. Recent work has shown that the presence of boundaries can significantly affect the behavior of waves in confined geometries. The presence of sharp corners may cause spiral nucleation from planar waves [40], while existing spirals are predicted to drift along the boundaries [41]. A number of experiments probe the dynamics of spirals near a boundary in the Belousov-Zhabotinsky reaction [42–44] and find a measurable force that leads to meandering drift along the boundary. The effect of domain size on rotating waves has recently been studied experimentally by Hartmann *et al.* [17] for the NO+CO reaction on a microstructured Pt(100) surface. The frequency of rotating waves was observed to increase substantially for domain sizes below a critical domain size (that depends on the spiral wavelength in large domains) due to the interaction of the wave tip with the boundary. A linear increase in the spiral frequency with inverse domain size was analytically predicted by Davydov and Zykov [14] and supported by numerical simulations [17]. Furthermore, close to the onset of appreciable frequency increase, a transition to quasiperiodic spirals was observed in simulations. After this transition, the spiral core is observed to drift near the boundary; we refer to this phenomenon as boundary-induced meandering. It is intimately linked to the boundary-induced drift studied in large domains [42–44]. Both phenomena result from the breaking of translational symmetry by the presence of a boundary.

The stability analysis performed here is for a spiral that rotates around the center of a circular domain. In this setup, small domains result in small distances between the center of rotation and the boundary. If the interaction with the boundary destabilizes the rotation of the spiral, we observe spiral tip trajectories that qualitatively closely resemble the ones found in meandering spirals in large domains. Hence, we chose the term boundary-induced meandering instead of boundary-induced drift. We used the model introduced in the preceding section. Time evolution of a suitable initial condition was performed to obtain an initial spiral wave for a circular domain of size  $R=5$  units. Dimensionless param-

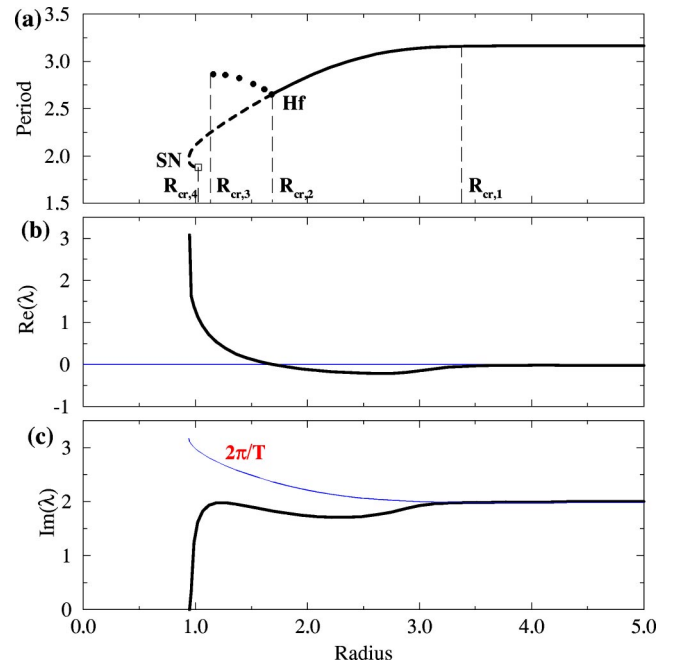


FIG. 2. Bifurcation diagram of a spiral wave in a circular domain with respect to the domain size. The period  $T$  is plotted as a function of the radius  $R$ . The parameters  $\epsilon$ ,  $a$ , and  $b$  are the same as in Fig. 1. A qualitative sketch of the branch of meandering spirals below the Hopf bifurcation  $H_f$  (as observed in direct numerical integrations) is given. The bottom two plots show the real and imaginary parts of the eigenvalue pair that, in infinite domains, is associated with the translational symmetry.

eters were taken in the typical excitable regime, as  $\epsilon=0.025$ ,  $a=0.8$ ,  $b=0.02$ . The wavelength of a spiral in a large domain for these conditions is about 9.1. Starting from an initial guess of the spiral and its period, steady state continuation of the spiral solution was performed using the domain size  $R$  as the bifurcation parameter.

The bifurcation diagram of the spiral solution branch is displayed in Fig. 2(a) where the spiral period is plotted against the domain size. Figures 2(b) and 2(c) display the real and imaginary parts of the eigenvalue pair that is associated with the translational symmetry of the spiral in the unbounded medium. When the domain size is above a critical value  $R_{cr,1}$ , the spiral frequency remains essentially independent of the domain size. Note that  $R_{cr,1}$  is less than half of the “large domain spiral wavelength,” in line with the observations in simulations of the standard Barkley model reported in Ref. [17]. Furthermore, the eigenvalues corresponding to the (broken) translational symmetry are indeed close to the translational eigenvalues for a spiral in an infinite medium,  $\lambda_T \approx 0 \pm i2\pi/T$ . Therefore, the value of  $R_{cr,1}$  gives a lower bound on the domain size above which the domain boundaries do not appreciably influence the spiral core.

For  $R < R_{cr,1}$  the spiral period is observed to decrease notably. As  $R$  decreases further, the eigenvalue pair associated with the broken translational symmetry  $\lambda_T$  is seen to move appreciably into the left half of the complex plane. There exists another critical radius  $R_{cr,2}$  such that for domain sizes in between the two limits ( $R_{cr,2} < R < R_{cr,1}$ ) the eigenvalue

pair  $\lambda_T$  lies in the stable region [ $\text{Re}(\lambda_T) < 0$ ]. In this regime, spirals that are either perturbed away from the center or initiated off-center are attracted towards the center of the domain. At  $R = R_{cr,2}$ , the eigenvalues that smoothly descend from the translational symmetry cross the imaginary axis into the right half plane indicating a Hopf bifurcation. The stable solution after this bifurcation is a quasiperiodic spiral. This Hopf bifurcation marks the onset of boundary-induced meandering.

We observed that the quasiperiodic spiral solution persists down to a certain cutoff domain size  $R_{cr,3}$  below which the medium does not support any stable rotating waves. The unstable spiral branch, when continued further down in  $R$  turns around in a saddle-node (SN) bifurcation at  $R_{SN}$  and then proceeds to collide with a spatially uniform steady state, namely, the one corresponding to the unstable focus, at some critical domain size  $R_{cr,4}$ , see Fig. 2(a). The latter result implies that for radii  $R$  with  $R_{SN} < R < R_{cr,4}$ , two unstable rotating wave solutions coexist. The lower branch separates the rest state of the medium from the upper spiral branch and is reminiscent of the recently observed unstable nucleus of a spiral pair in large domains [45].

V. TRANSITION TO MEANDERING SPIRALS

We demonstrated in the preceding section that the influence of the boundaries in smaller domains causes a quasiperiodic instability of the spiral core. The eigenmodes corresponding to this instability are the ones originating from breaking the translational symmetry of the spirals in an unbounded domain. We refer to this instability as boundary-induced meandering. Spirals in extended domains are known to exhibit another qualitatively different type of transition to quasiperiodic motion. Barkley [7] showed that this “infinite domain” meandering transition is caused by a Hopf bifurcation of a set of isolated eigenvalues (that are *different* from the eigenvalues corresponding to the translational invariance). This instability will be referred to as “regular meandering” or just “meandering.” The eigenvector corresponding to the regular meandering instability was shown to decay radially outward [7]. The bifurcations that give rise to the two different instabilities will be termed boundary Hopf ( $H_b$ ) and meandering Hopf ( $H_m$ ), respectively. The meandering-Hopf transition also causes a quasiperiodic motion of the spiral tip which exhibits complex flowerlike motions in the domain.

Figure 3 shows the bifurcation scenario of the spiral solution in a circular domain keeping  $R = 5$  constant and using  $\epsilon$  as the control parameter. The remaining parameters are fixed as before at  $a = 0.8$ ,  $b = 0.02$ . The stable spiral branch has a Hopf bifurcation (marked as  $H_m$  in Fig. 3) as  $\epsilon$  is increased beyond a critical value where an isolated complex eigenpair crosses into the right half plane. A stable branch of meandering spirals arises at this Hopf bifurcation. At a slightly higher value of  $\epsilon$ , the meandering branch retracts and disappears via another Hopf bifurcation as the isolated pair of eigenvalues returns to the left half plane. The spiral solution is then stable for a narrow interval in  $\epsilon$ . The spiral period increases monotonically for increasing  $\epsilon$  and the

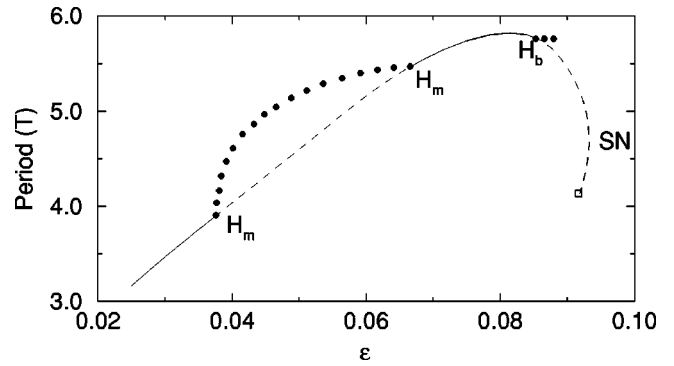


FIG. 3. Bifurcation diagram of a spiral wave solution for  $R = 5$ ,  $a = 0.8$ ,  $b = 0.02$ . The solid and dashed lines indicate stable and unstable spirals. The filled circles denote quasiperiodic spirals while the unfilled square denotes a spatially uniform state. The symbols  $H_b$ ,  $H_m$ , and SN stand for boundary-Hopf, meandering-Hopf, and saddle-node bifurcations, respectively.

boundaries of the domain start eventually to affect the spiral core. This causes the complex eigenvalue pair associated with the broken translational symmetry to move *away* from the imaginary axis into the left half plane. At this point, spirals that are kicked off the center, or initiated off-center, are attracted towards the middle of the domain. At the point marked as  $H_b$  in Fig. 3, the eigenpair associated with the broken translational symmetry crosses the imaginary axis into the unstable right half plane causing the boundary-induced meandering of the spiral. The unstable spiral branch when continued further up in  $\epsilon$  turns around in a saddle-node bifurcation and terminates at a spatially uniform steady state of the system at some critical value of  $\epsilon$ . This uniform state

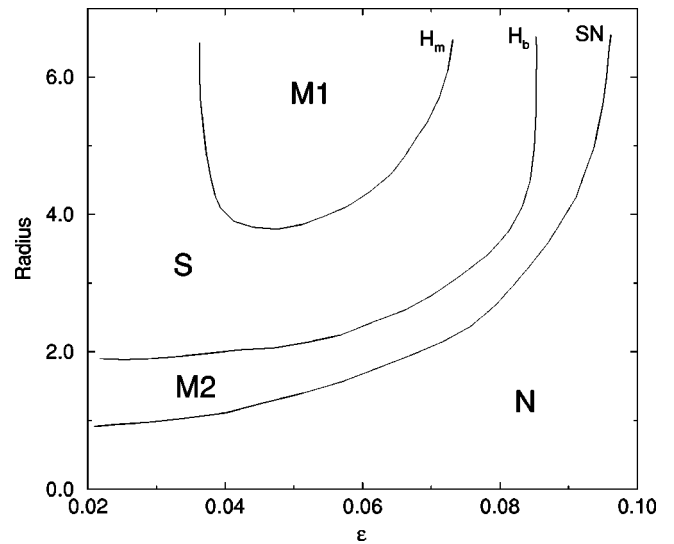


FIG. 4. Two-parameter numerical bifurcation diagram of rotating spiral waves in finite domains. The curves  $H_m$ ,  $H_b$ , and SN represent the meandering-Hopf bifurcation, the boundary-induced meandering related Hopf bifurcation, and saddle node of spirals, respectively. The  $H_m$  and  $H_b$  curves define the critical radii  $R_{cr,0}$  and  $R_{cr,2}$ . The variously marked regions support stable spirals (S), regular meandering spirals (M1), boundary-induced meandering spirals (M2), and no rotating waves (N).

corresponds to an unstable fixed point in the local dynamics.

Next we free both the parameters  $\epsilon$  and  $R$  in the model and study how the two Hopf transitions are organized in the  $(\epsilon, R)$  parameter space. The two-parameter bifurcation diagram is displayed in Fig. 4, and was assembled by performing several one-parameter continuation runs at both constant  $R$  and constant  $\epsilon$  cuts. The curves corresponding to the meandering-Hopf bifurcation, the boundary-Hopf bifurcation, and saddle node of spirals are marked as  $H_m$ ,  $H_b$ , and SN, respectively. The regions represent stable rotating spirals ( $S$ ), regular meandering spirals (M1), boundary-induced meandering spirals (M2), and no rotating waves ( $N$ ), respectively. These results show that regular meandering is suppressed by the influence of the boundary conditions upon decreasing the domain radius. At still smaller domain radii, boundary-induced meandering appears.

## VI. DISCUSSION

We have studied computationally certain features of the dynamics of rotating spirals in small two-dimensional domains by numerical bifurcation and stability analysis. Following Barkley's earlier work [7], we found that these spirals rotate around the center of a circular domain and computed them as steady states of the reaction-diffusion equations in a corotating frame. The stability is inferred from an iterative determination of the largest eigenvalues of the equations lin-

earized around the spiral solution. For large domains, we obtain three eigenvalues with practically zero real part, a real one for rotation symmetry and a complex conjugate pair for (slightly broken) translational symmetry in the plane. For decreasing domain size, the real part of the complex conjugate pair becomes negative, indicating a repulsive interaction with the (mirror) boundary. At even smaller domain sizes, the real part starts to grow and finally becomes positive indicating a boundary-induced meandering instability. Furthermore, it was observed that regular meandering in large domains can be suppressed due to boundary effects. At the parameter values bounding their existence, spirals were observed to disappear in saddle-node bifurcations.

Numerical stability analysis of spirals in circular domains is useful in quantifying the interaction between a spiral and the domain boundary. This can lead to a better understanding of the instabilities and bifurcations of spirals in small domains. Similar computer-assisted studies might be helpful in analyzing related problems, such as the interaction of a spiral pair in a small domain (as observed by Hartmann *et al.* [18] in a catalytic surface reaction).

## ACKNOWLEDGMENTS

This work was partially supported by the National Science Foundation. I.G.K. also wishes to acknowledge a Humboldt Foundation Forschungspreis.

- 
- [1] V.S. Zykov, *Biophysics* (Engl. Transl.) **31**, 862 (1986).
  - [2] A.T. Winfree, *Chaos* **1**, 303 (1991).
  - [3] A.S. Mikhailov and V.S. Zykov, *Physica D* **52**, 379 (1991).
  - [4] A. Karma, *Chaos* **4**, 461 (1994).
  - [5] J.P. Keener and J.J. Tyson, *Physica D* **21**, 300 (1986).
  - [6] D.A. Kessler and H. Levine, *Physica D* **49**, 90 (1991).
  - [7] D. Barkley, *Phys. Rev. Lett.* **68**, 2090 (1992).
  - [8] S.C. Müller, T. Plesser, and B. Hess, *Science* **230**, 661 (1985).
  - [9] G.S. Skinner, and H.L. Swinney, *Physica D* **48**, 1 (1990).
  - [10] S. Nettesheim, A. von Oertzen, H.H. Rotermund, and G. Ertl, *J. Chem. Phys.* **98**, 9977 (1993).
  - [11] S. Rica and E. Tirapegui, *Phys. Rev. Lett.* **64**, 878 (1990).
  - [12] C. Elphick and E. Meron, *Physica D* **53**, 385 (1991).
  - [13] I.S. Aranson, L. Kramer, and A. Weber, *Phys. Rev. E* **47**, 3231 (1993).
  - [14] V.A. Davydov and V.S. Zykov, *Zh. Eksp. Teor. Fiz.* **76**, 414 (1993).
  - [15] I.S. Aranson, D. Kessler, and I. Mitkov, *Phys. Rev. E* **50**, R2395 (1994).
  - [16] A. K. Bangia, Ph.D. thesis, Princeton University, 1997.
  - [17] N. Hartmann, M. Bär, I.G. Kevrekidis, K. Krischer, and R. Imbihl, *Phys. Rev. Lett.* **76**, 1384 (1996).
  - [18] N. Hartmann, I.G. Kevrekidis, and R. Imbihl, *J. Chem. Phys.* **112**, 6795 (2000).
  - [19] P.C. Fife, *J. Stat. Phys.* **39**, 687 (1985).
  - [20] A. Bernoff, *Physica D* **53**, 125 (1991).
  - [21] P. Pelcé and J. Sun, *Physica D* **48**, 353 (1991).
  - [22] P. Pelcé and J. Sun, *Physica D* **63**, 273 (1993).
  - [23] A. Karma, *Phys. Rev. Lett.* **68**, 397 (1992).
  - [24] D. Kessler and R. Kupferman, *Physica D* **97**, 509 (1996).
  - [25] D. Margerit and D. Barkley, *Phys. Rev. Lett.* **86**, 175 (2001).
  - [26] N. Wiener and A. Rosenblueth, *Arch. Inst. Cardiol. Mex.* **16**, 205 (1946).
  - [27] V. S. Zykov, *Simulation of Wave Processes in Excitable Media* (Manchester University Press, New York, 1987).
  - [28] D. Barkley, *Physica D* **49**, 61 (1991).
  - [29] A. Karma, *Phys. Rev. Lett.* **65**, 2824 (1990).
  - [30] A.M. Pertsov, A.V. Panfilov, and E.A. Ermakova, *Physica D* **14**, 117 (1984).
  - [31] M. Bär and M. Eiswirth, *Phys. Rev. E* **48**, R1635 (1993).
  - [32] M. Bär, N. Gottschalk, M. Eiswirth, and G. Ertl, *J. Chem. Phys.* **100**, 1202 (1994).
  - [33] D. Barkley, in *Chemical Waves and Patterns*, edited by K. Showalter and R. Kapral (Kluwer, Dordrecht, 1995).
  - [34] D. Barkley, *Phys. Rev. Lett.* **72**, 164 (1994).
  - [35] J.R. Leis and M.A. Kramer, *ACM Trans. Math. Softw.* **14**, 61 (1988).
  - [36] Y. Saad, *Numerical Methods for Large Eigenvalue Problems* (Manchester University Press, Manchester, 1992).
  - [37] I. Goldhirsch, S.A. Orszag, and B.K. Maulik, *J. Sci. Comput.* **2**, 33 (1987).
  - [38] K.N. Christodoulou and L.E. Scriven, *J. Sci. Comput.* **3**, 355 (1988).
  - [39] Y. Saad and M.H. Schultz, *SIAM (Soc. Ind. Appl. Math.) J. Sci. Stat. Comput.* **7**, 856 (1986).

- [40] K. Agladze, J.P. Keener, S.C. Müller, and A. Panfilov, *Science* **264**, 1746 (1994).
- [41] J.A. Sepulchre and A. Babloyantz, *Phys. Rev. E* **48**, 187 (1993).
- [42] S. C. Müller and V. S. Zykov, in *Dynamical Phenomena in Living Cells*, edited by E. Moseskilde and O. G. Mouritsen (Springer, Berlin, 1995).
- [43] M. Gomez-Gesteira, A.P. Munuzuri, V. Perez-Munuzuri, and V. Perez-Villar, *Phys. Rev. E* **53**, 5480 (1996).
- [44] H. Brandstädter, M. Braune, I. Schebesch, and H. Engel, *Chem. Phys. Lett.* **323**, 145 (2000).
- [45] E. Mihaliuk, T. Sakurai, F. Chirila, and K. Showalter, *Phys. Rev. E* **65**, 065602 (2002).